

Mechanism of transverse viscous transport in classical solids

Akira Furukawa*

Institute of Industrial Science, University of Tokyo, Meguro-ku, Tokyo 153-8505, Japan

(Dated: November 15, 2019)

We propose a possible mechanism of transverse viscous transport in solid-state systems. Time integration of the Eulerian velocity field shows definite diffusive behavior caused by a cumulative deviation from the true displacement field. This diffusive behavior can be further attributed to the length-scale-dependent viscous momentum-transfer mechanism, which is not associated with any significant material flows or displacements and is thus essentially different from that in ordinary liquids. The validity of the present argument is verified by classical molecular dynamics simulations of deeply supercooled liquids, glasses, and crystalline solids.

Viscosity, which characterizes flow resistance, is one of the most fundamental transport properties of liquids [1]. In elastic solids, on the other hand, although the importance of viscosity has frequently been considered [2], we still do not fully understand its role and mechanism. The general question is: how can momentum be transferred without material flow?

To answer this question, in this paper, we mainly focus on the viscosity problem in glassy liquids. Glassy materials exhibit both liquid- and solid-like mechanical properties depending on the observed time scale [3, 4]. For time scales smaller than the structural relaxation time, τ_α , the mechanical response is elastic, while for time scales larger than τ_α , a liquid-like viscous response is observed. Therefore, the structural relaxation time τ_α determines the solid-to-liquid crossover, and the macroscopic viscosity η can be described as $\eta \cong G\tau_\alpha$ [5], where G is the shear elastic modulus. However, the situation is more complicated than this simple picture because viscous transport has been shown to also strongly depend on the length scale [6–9]: at smaller length scales (see below), the viscosity is much smaller than the macroscopic value. Furthermore, the crossover from the elastic response to the viscous response occurs at time scales much smaller than τ_α [9], indicating that viscous transport is dominant well before significant flows or particle rearrangements occur. In this paper, we demonstrate that such viscous momentum transfer can be realized.

First, we study the length-scale-dependent elastic-to-viscous crossover by analyzing the spatial correlation of the “displacement” field of a model glass former [10, 11] using classical molecular dynamics simulations [12]. The details of the simulations and the model are presented in Appendix. The displacement field for a time duration of Δt is defined in Fourier space as follows. (i) The displacement field for specific positions of particles is usually defined as

$$\hat{\mathbf{u}}_{\mathbf{k}}(\Delta t) = \frac{1}{\sqrt{N}} \sum_{\lambda=1}^N \int_0^{\Delta t} dt' \mathbf{v}_\lambda(t') e^{-i\mathbf{k} \cdot \mathbf{r}_\lambda^*}, \quad (1)$$

where N is the total number of particles and \mathbf{k} is the wave vector. In the following, we set the reference positions $\{\mathbf{r}_\lambda^*\}$ for the particle positions at $t = 0$, $\{\mathbf{r}_\lambda(0)\}$ [13]. Here, $\mathbf{r}_\lambda(t)$ and $\mathbf{v}_\lambda(t)$ are the position and velocity of the λ -th particle at time t , respectively. Otherwise, when investigating the displacement behavior for $\Delta t \lesssim \tau_\alpha$, we may use the time-averaged [14] or inherent-state positions as $\{\mathbf{r}_\lambda^*\}$ instead of $\{\mathbf{r}_\lambda(0)\}$. (ii) Alternatively, the displacement field may be defined as:

$$\begin{aligned} \mathbf{u}_{\mathbf{k}}(\Delta t) &= \frac{1}{\sqrt{N}} \sum_{\lambda=1}^N \int_0^{\Delta t} dt' \mathbf{v}_\lambda(t') e^{-i\mathbf{k} \cdot \mathbf{r}_\lambda(t')} \\ &= \int_0^{\Delta t} dt' \mathbf{v}_{\mathbf{k}}(t'), \end{aligned} \quad (2)$$

where $\mathbf{v}_{\mathbf{k}}(t)$ is the velocity field [15].

In Fig. 1, we show $\hat{S}(k; \Delta t) = \langle |\hat{\mathbf{u}}_{\mathbf{k}}^\perp(\Delta t)|^2 \rangle$ and $S(k; \Delta t) = \langle |\mathbf{u}_{\mathbf{k}}^\perp(\Delta t)|^2 \rangle$ for various Δt in a supercooled state, where $\hat{\mathbf{u}}_{\mathbf{k}}^\perp$ and $\mathbf{u}_{\mathbf{k}}^\perp$ are the transverse components of $\hat{\mathbf{u}}_{\mathbf{k}}$ and $\mathbf{u}_{\mathbf{k}}$, respectively. Hereafter, $\langle \dots \rangle$ denotes an ensemble average. We find that $\hat{S}(k; \Delta t)$ and $S(k; \Delta t)$ behave quite differently, except for at a very small Δt . For $t_s \ll \Delta t \ll \tau_\alpha$, where t_s is the time for the transverse sound to propagate across the length of the system, $i\mathbf{k}\hat{\mathbf{u}}_{\mathbf{k}}^\perp + (i\mathbf{k}\hat{\mathbf{u}}_{\mathbf{k}}^\perp)^\dagger$ can be approximately regarded as thermally fluctuating elastic shear strain. Therefore, for such Δt [16, 17],

$$\hat{S}(k; \Delta t) \cong \frac{2T}{k^2 G(k)}, \quad (3)$$

where T is the temperature measured in units of Boltzmann’s constant and $G(k)$ is the k -dependent shear elastic modulus. For a smaller k , $G(k)$ approaches its macroscopic value G , resulting in the k^{-2} dependence of $\hat{S}(k; \Delta t)$ [13, 14, 18–21]. On the other hand, $S(k; \Delta t)$ behaves in a completely different way: although, for smaller Δt and k , $S(k; \Delta t)$ behaves similarly to $\hat{S}(k; \Delta t)$, with increasing Δt , the difference between $S(k)$ and $\hat{S}(k)$ becomes more pronounced at larger k . We can ascribe this behavior of $S(k; \Delta t)$ to the length-scale-dependent elastic-to-viscous crossover as follows. $S(k; \Delta t)$ can be

*furu@iis.u-tokyo.ac.jp

generally related to the velocity autocorrelation as

$$S(k; \Delta t) = \int_0^{\Delta t} ds \int_0^{\Delta t} ds' \langle \mathbf{v}_{\mathbf{k}}^\perp(s) \cdot \mathbf{v}_{-\mathbf{k}}^\perp(s') \rangle. \quad (4)$$

From the definition of the k -dependent viscosity $\eta(k)$ [22, 23], for a sufficiently large Δt , $S(k; \Delta t)$ follows (see Appendix)

$$S(k; \Delta t) \cong \Delta t \frac{4T}{k^2 \eta(k)}. \quad (5)$$

At a length scale of $\sim 1/k$, the crossover from the elastic response [Eq. (3)] to the viscous response [Eq. (5)] occurs at approximately $\Delta t \sim \tau(k) \equiv \eta(k)/G(k)$, which describes the generalized Maxwell relation and can also be observed in the complex shear modulus [9]. Finding such a qualitative difference may be surprising, because these two definitions, Eqs. (1) and (2), have been thought to be physically equivalent as long as most particles remain around their original positions. However, as clearly shown in Fig. 1, this is not the case: for $\Delta t \ll \tau_\alpha$, $\hat{\mathbf{u}}_{\mathbf{k}}(\Delta t)$ represents the collective vibrational fluctuations, while $\mathbf{u}_{\mathbf{k}}(\Delta t)$ undergoes diffusive behavior controlled by the length-scale-dependent viscosity $\eta(k)$. This difference can be ascribed to the cumulative deviation between $\mathbf{u}_{\mathbf{k}}(\Delta t)$ and the true displacement field [15].

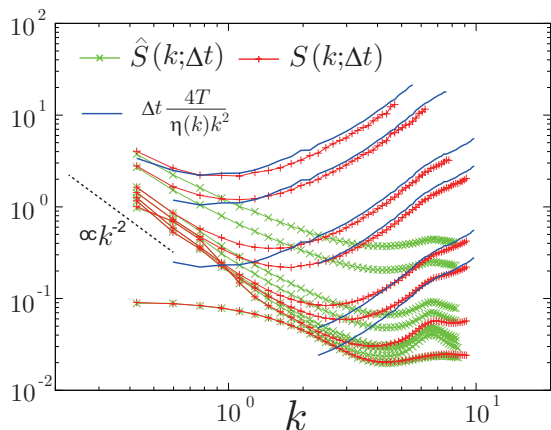


FIG. 1: (Color online) $\hat{S}(k; \Delta t)$ (green curve) and $S(k; \Delta t)$ (red curve) in a supercooled state ($T = 0.275$) at $\Delta t/\tau_\alpha = 5 \times 10^{-4}, 2 \times 10^{-3}, 10^{-2}, 2 \times 10^{-2}, 10^{-1}, 2 \times 10^{-1}, 1$, and 2 (from bottom to top). Here, τ_α is defined as the macroscopic shear-stress relaxation time. The blue curve represents $\Delta t[4T/\eta(k)k^2]$, where $\eta(k)$ is given in Fig. 4. At $\Delta t = 5 \times 10^{-4}\tau_\alpha$, $\hat{S}(k; \Delta t)$ and $S(k; \Delta t)$ collapse onto each other. However, with increasing Δt , the difference between $\hat{S}(k; \Delta t)$ and $S(k; \Delta t)$ increases.

The physical significance of the observed diffusive behavior of $\mathbf{u}_{\mathbf{k}}(\Delta t)$ can be viewed from a slightly different perspective. For this purpose, let us assume a hypothetical cubic box \mathcal{V}_ℓ of linear dimension ℓ in a system and define two types of box-averaged “displacements”: $\hat{\mathbf{U}}_\ell(\Delta t) = \int_0^{\Delta t} dt' \hat{\mathbf{V}}_\ell(t')$ and $\mathbf{U}_\ell(\Delta t) = \int_0^{\Delta t} dt' \mathbf{V}_\ell(t')$

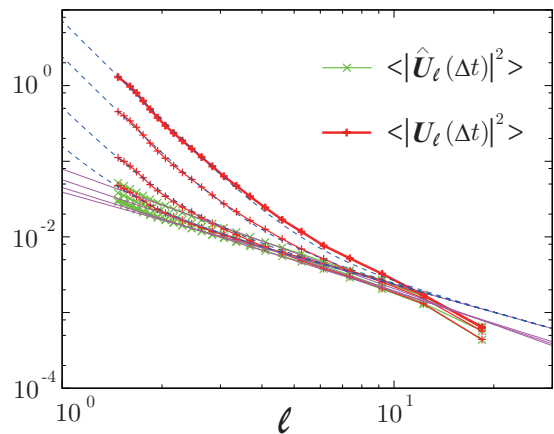


FIG. 2: (Color online) $\langle |\hat{\mathbf{U}}_\ell(\Delta t)|^2 \rangle$ and $\langle |\mathbf{U}_\ell(\Delta t)|^2 \rangle$ as a function of ℓ in a supercooled state ($T = 0.267$) at $\Delta t/\tau_\alpha = 10^{-3}, 4 \times 10^{-3}, 2 \times 10^{-2}$, and 6×10^{-2} (from bottom to top). For $\Delta t \ll \tau_\alpha$, $\langle |\hat{\mathbf{U}}_\ell(\Delta t)|^2 \rangle$ remains almost unchanged. The purple curves are fits to $\langle |\hat{\mathbf{U}}_\ell(\Delta t)|^2 \rangle$, $f_0(\ell, \Delta t) \cong A\ell^b$, where the coefficient A and the exponent b (~ -1 ; due to elasticity [24]) slightly depend on Δt . However, $\langle |\mathbf{U}_\ell(\Delta t)|^2 \rangle$ exhibits diffusive behavior. The dashed curve represents $f_0(\ell, \Delta t) + g(\ell)\Delta t$, where $g(\ell) = 0.024\ell^{-4.4}$ fitted to $\langle |\mathbf{U}_\ell(\Delta t)|^2 \rangle$.

with $\hat{\mathbf{V}}_\ell(t)$ and $\mathbf{V}_\ell(t)$ being

$$\hat{\mathbf{V}}_\ell(t) = \frac{1}{N_\ell(0)} \sum_{\{\mathbf{r}_\lambda(0)\} \in \mathcal{V}_\ell} \mathbf{v}_\lambda(t) \quad (6)$$

and

$$\mathbf{V}_\ell(t) = \frac{1}{N_\ell(t)} \sum_{\{\mathbf{r}_\lambda(t)\} \in \mathcal{V}_\ell} \mathbf{v}_\lambda(t), \quad (7)$$

respectively, where $N_\ell(t)$ ($\sim \rho \ell^d$) is the number of particles in the box \mathcal{V}_ℓ at time t , ρ is the number density, and d is the spatial dimensionality (here, $d = 3$). In Eq. (6), the sum is taken over particles whose positions at $t = 0$ are within the box. On the other hand, in Eq. (7), particles over which the sum is taken depends on t . In Fig. 2, we plot $\langle |\hat{\mathbf{U}}_\ell(\Delta t)|^2 \rangle$ and $\langle |\mathbf{U}_\ell(\Delta t)|^2 \rangle$ as a function of ℓ for various Δt in a supercooled state. For $\Delta t \ll \tau_\alpha$, although $\langle |\hat{\mathbf{U}}_\ell(\Delta t)|^2 \rangle$ remains approximately unchanged, $\langle |\mathbf{U}_\ell(\Delta t)|^2 \rangle$ linearly grows with Δt for a smaller ℓ . We emphasize that $\hat{\mathbf{U}}_\ell(\Delta t)$ is the average displacement of particles selected at $t = 0$, similar to $\hat{\mathbf{u}}_{\mathbf{k}}(\Delta t)$, whereas $\mathbf{U}_\ell(\Delta t)$ is determined by particles that move through the box at some time during the period $[t, t + \Delta t]$, similar to $\mathbf{u}_{\mathbf{k}}(\Delta t)$. Thus, we may consider that the observed qualitative difference between $\langle |\hat{\mathbf{U}}_\ell(\Delta t)|^2 \rangle$ and $\langle |\mathbf{U}_\ell(\Delta t)|^2 \rangle$ has the same origin as that between $\hat{S}(k; \Delta t)$ and $S(k; \Delta t)$.

To understand the diffusive behavior of $\langle |\mathbf{U}_\ell(\Delta t)|^2 \rangle$, let us consider a particle (number: λ) located close to the box boundary, which for $\Delta t \ll \tau_\alpha$ oscillates around its inherent-state position and repeatedly crosses the boundary surface. The net displacement inside the box \mathcal{V}_ℓ for

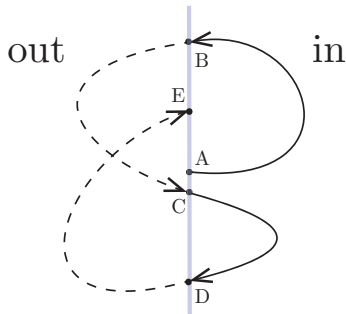


FIG. 3: (Color online) Schematic of the short-term ($\ll \tau_\alpha$) trajectory of a particle that is randomly oscillating around the boundary of \mathcal{V}_ℓ represented by the light blue line. For this trajectory, the net displacement inside \mathcal{V}_ℓ is $\vec{AB} + \vec{CD}$, which is parallel to the boundary surface (the perpendicular component is 0). The mean turnover time for the particle momentum is approximately given by $1/\omega_0$, where ω_0 is the mean frequency of the particle oscillation.

the duration Δt , $\mathbf{X}_\lambda(\Delta t)$ is given by

$$\mathbf{X}_\lambda(\Delta t) = \sum_{p=1}^M [\mathbf{r}_\lambda(t_p^{(\text{out})}) - \mathbf{r}_\lambda(t_p^{(\text{in})})] : \quad (8)$$

The particle crosses into and subsequently out of the box at $t = t_p^{(\text{in})}$ and $t = t_p^{(\text{out})}$, respectively, and the particle displacement between the two crossing events, $\mathbf{r}_\lambda(t_p^{(\text{out})}) - \mathbf{r}_\lambda(t_p^{(\text{in})})$, is parallel to the box boundary (the perpendicular component is zero). As discussed below, this difference between the parallel and perpendicular components causes different behaviors of the displacement correlation between the transverse and longitudinal modes. We suppose that for the duration Δt , such crossings happen $2M$ times. $M \sim \Delta t \omega_0$, with ω_0 being the mean frequency of this oscillation. Assuming that the crossing events occur almost randomly, the average of $\mathbf{X}_\lambda(\Delta t)$ is zero, and the mean deviation is approximately given as

$$\begin{aligned} \langle |\mathbf{X}_\lambda(\Delta t)|^2 \rangle &\sim M \langle |\mathbf{r}_\lambda(t_p^{(\text{out})}) - \mathbf{r}_\lambda(t_p^{(\text{in})})|^2 \rangle \\ &\sim \Delta t \omega_0 a^2, \end{aligned} \quad (9)$$

where a is the mean oscillation amplitude, namely, $\langle |\mathbf{r}_\lambda(t_p^{(\text{out})}) - \mathbf{r}_\lambda(t_p^{(\text{in})})|^2 \rangle \sim a^2$. This situation is schematically shown in Fig. 3. Particles around the box surface almost independently [27] contribute to the diffusive behavior of \mathbf{U}_ℓ . The number of such particles is approximately $\rho \ell^{d-1} a$. Therefore, we obtain the diffusion coefficient of \mathbf{U}_ℓ as

$$D_\ell \sim \frac{a^3 \omega_0}{\rho \ell^{d+1}}, \quad (10)$$

which is consistent with the simulation results shown in Fig. 2: at $T = 0.267$ and $\rho = 0.8$, a is approximately three-tenths of the particle size (\sim the Lindemann length) and $\omega_0 \sim \sqrt{T/m_\lambda a^2} \sim \mathcal{O}(1)$, where m_λ is the particle mass, leading to $D_\ell \sim 10^{-2} \ell^{-4}$.

This diffusion coefficient can be related to the autocorrelation of $\mathbf{V}_\ell(t)$ as

$$D_\ell \cong 2 \int_0^{t_d} dt \langle \mathbf{V}_\ell(t) \cdot \mathbf{V}_\ell(0) \rangle \quad (11)$$

with a sufficiently long integration time of t_d . We decompose $\mathbf{V}_\ell(t)$ into two parts: $\mathbf{V}_\ell(t) = \mathbf{V}_\ell^{(0)}(t) + \partial \mathbf{V}_\ell(t)$, where

$$\mathbf{V}_\ell^{(0)}(t) = \frac{1}{N_\ell(t)} \sum_{\{\mathbf{r}_\lambda(t)\} \in \mathcal{V}_\ell - \partial \mathcal{V}_\ell} \mathbf{v}_\lambda(t), \quad (12)$$

and

$$\partial \mathbf{V}_\ell(t) = \frac{1}{N_\ell(t)} \sum_{\{\mathbf{r}_\lambda(t)\} \in \partial \mathcal{V}_\ell} \mathbf{v}_\lambda(t). \quad (13)$$

Here, $\partial \mathcal{V}_\ell$ represents the inner surface region (width $\sim a$) of the box \mathcal{V}_ℓ . For $\Delta t \ll \tau_\alpha$, the particles mainly belonging to $\partial \mathcal{V}_\ell$ oscillate across the boundary, while the particles in $\mathcal{V}_\ell - \partial \mathcal{V}_\ell$ oscillate around their inherent-state positions without crossing the boundary and thus do not contribute to D_ℓ . Then, the integration of Eq. (11) can be rewritten as

$$\begin{aligned} D_\ell &\cong \int_0^{1/\omega_0} dt \langle \partial \mathbf{V}_\ell(t) \cdot \partial \mathbf{V}_\ell(0) \rangle \\ &\sim \frac{1}{\omega_0} \langle |\partial \mathbf{V}_\ell|^2 \rangle \sim \frac{a^3 \omega_0}{\rho \ell^{d+1}}, \end{aligned} \quad (14)$$

which is consistent with Eq. (10). Here, we assume that the randomization time of the velocity $\partial \mathbf{V}_\ell(t)$ is approximately $1/\omega_0$, and the equipartition law gives $\langle |\partial \mathbf{V}_\ell|^2 \rangle \sim (a^3 \omega_0^2 / \rho \ell^{d+1})$.

We have thus far argued that the random particles' motion around the boundary of \mathcal{V}_ℓ gives rise to the diffusive behavior of $\mathbf{U}_\ell(\Delta t)$. Furthermore, Eqs. (11)-(14) indicate that the irreversible momentum exchanges between inside and outside of \mathcal{V}_ℓ underlie this diffusivity. As shown below, such momentum exchanges can be related to the length-scale-dependent viscosity. The time evolution of the momentum defined by $\mathbf{J}_\ell(t) = \sum_{\{\mathbf{r}_\lambda(t)\} \in \mathcal{V}_\ell} m_\lambda \mathbf{v}_\lambda(t) = \int_{\mathcal{V}_\ell} d\mathbf{r} \mathbf{j}(\mathbf{r}, t)$, where $\mathbf{j}(\mathbf{r}, t)$ is the momentum field, which is formally described as

$$\begin{aligned} \frac{d}{dt} \mathbf{J}_\ell(t) &= \int_{\mathcal{V}_\ell} d\mathbf{r} \nabla \cdot \overset{\leftrightarrow}{\boldsymbol{\sigma}}(\mathbf{r}, t) \\ &= \int_{\mathcal{S}_\ell} dS \hat{\mathbf{n}}_\ell \cdot \overset{\leftrightarrow}{\boldsymbol{\sigma}}(\mathbf{r}, t) \\ &= - \int_{-\infty}^t dt' \zeta_\ell(t-t') \mathbf{J}_\ell(t') + \boldsymbol{\theta}_\ell(t). \end{aligned} \quad (15)$$

The first and second lines represent momentum conservation, where $\overset{\leftrightarrow}{\boldsymbol{\sigma}}(\mathbf{r}, t)$ is the stress tensor at time t and position \mathbf{r} . In the second line, the integration is performed over the box surface \mathcal{S}_ℓ , and $\hat{\mathbf{n}}_\ell$ is the outward normal unit vector to \mathcal{S}_ℓ . The third line in Eq.

(15) is the generalized Langevin equation, where $\zeta_\ell(t)$ is the memory kernel representing both the elasticity and the friction [28], and $\theta_\ell(t)$ is the noise term. In frequency (ω) space, the memory kernel is expressed as $\hat{\zeta}_\ell(\omega) = \int_0^\infty dt e^{-i\omega t} \zeta_\ell(t)$, and in the low-frequency limit ($\omega \rightarrow 0$), we obtain $\bar{M}_\ell \hat{\zeta}_\ell(0) \sim T/D_\ell$, where \bar{M}_ℓ is the time-averaged mass of the box. $\bar{M}_\ell \hat{\zeta}_\ell(0)$ is the friction coefficient of the long-time-scale dynamics. Equation (15) describes that the momentum exchange between the inner and outer regions consists of excitation and dissipation, resulting in the ‘‘Brownian motion’’ of $\mathbf{U}_\ell(\Delta t)$ (and of $\mathbf{u}_\mathbf{k}(\Delta t)$). Notably, this Brownian motion does not apply to the material (element) itself. In 3D, by expressing $\bar{M}_\ell \hat{\zeta}_\ell(0)$ in terms of the Stokes friction as $\bar{M}_\ell \hat{\zeta}_\ell(0) \sim \eta_\ell \ell$, we obtain the length-scale-dependent shear viscosity η_ℓ as

$$\eta_\ell \sim \frac{T}{\ell D_\ell} \sim \frac{\rho T}{a^3 \omega_0} \ell^3. \quad (16)$$

The wavenumber-dependent shear viscosity $\eta(k)$ may be defined as η_ℓ for $k \sim 1/\ell$, resulting in $\eta(k) \sim (\rho T/a^3 \omega_0) k^{-3}$, which is consistent with the numerical results shown in Fig. 4.

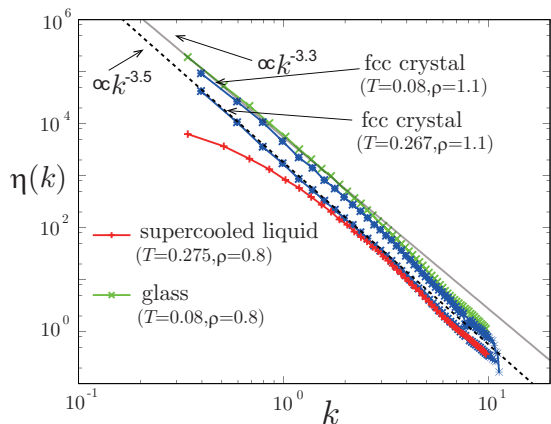


FIG. 4: (Color online) $\eta(k)$ for various states. In a supercooled liquid ($T = 0.275$), $\eta(k)$ shows a characteristic length scale of ξ_η [7, 9], and $\eta(k)$ approaches its macroscopic value for $k\xi_\eta \lesssim 1$. On the other hand, in solid-state materials (glass and crystal), no characteristic length exists, and $\eta(k) \sim k^c$, where the exponent c is close to -3 over the whole k range of the present study, which agrees with Eq. (16). For a glass, $T = 0.08$ is well below the Vogel-Fulcher-Tamman temperature ($T \approx 0.22$) [25].

Up to this point, for supercooled liquids ($\Delta t \lesssim \tau_\alpha$), we have presented an argument for the ‘‘Brownian’’ dynamics of $\mathbf{U}_\ell(\Delta t)$ and its underlying transverse viscous dissipation. However, our argument does not rely on specific properties of supercooled liquids: we have only assumed that the particles are oscillating around their original positions (or inherent-state positions) for time scales sufficiently smaller than τ_α . Therefore, we expect that the present argument is more general and applicable to other solid-state materials. In Fig. 4, we show

the wavenumber-dependent shear viscosity $\eta(k)$ for glass and crystalline solids as well as for a supercooled liquid. Please see Appendix for details of the simulations and the models. These plots clearly exhibit similar significant wavenumber dependence. Furthermore, note that our preliminary simulations for glasses and crystals (not shown here) also show essentially the same diffusive behaviors of $\mathbf{u}_\mathbf{k}(\Delta t)$ and $\mathbf{U}_\ell(\Delta t)$ as those shown in Figs. 1 and 2, respectively. Based on these results, we can conclude that $\eta(k)$ generally characterizes the transverse viscous dissipation not only in liquids but also in solids.

As shown in Fig. 5 of Ref. [9], in supercooled states, the characteristic length scale of the viscous transport, ξ_η , is determined from $\eta(k)$: for $k\xi_\eta \lesssim 1$, $\eta(k) \sim \eta$ ($\tau(k) \sim \tau_\alpha$), while for $k\xi_\eta \gtrsim 1$, $\eta(k)$ exhibits marked k -dependence. ξ_η increases with an increasing degree of supercooling, apparently indicating a close link between ξ_η and the dynamic heterogeneity [7, 9, 26]. However, this may not be the case. In $S(k; \Delta t)$, as Δt elapses, the elastic-to-viscous crossover gradually proceeds from larger k . Then, at $\Delta t \sim \tau_\alpha$, macroscopic structural rearrangement (*solid-to-liquid* crossover) occurs: at this Δt , the elastic transverse response is retained for $k\xi_\eta \lesssim 1$, but for $\Delta t > \tau_\alpha$, the response is viscous over the whole k . Therefore, ξ_η may be related to the macroscopic solid-to-liquid crossover at $\Delta t \sim \tau_\alpha$ but not to the dynamic heterogeneity. Note that this physical picture is different from that discussed in Refs. [7, 9, 26]. On the other hand, in solid-state materials, because no structural relaxation occurs, in $S(k; \Delta t)$, the elastic-to-viscous crossover indefinitely continues from smaller k with increasing Δt : neither a plateau nor a characteristic length scale exists in $\eta(k)$.

In summary, we proposed a possible mechanism of transverse viscous transport in solid-state systems with a particular focus on the length-scale-dependent shear viscosity in supercooled liquids. The mechanism proposed here is not associated with any significant material flows or structural rearrangements and is thus qualitatively different from that in ordinary liquids. For (transverse) hydrodynamic modes in solids, even without material flows, there should be dissipation channels as opposed to the energy injection due to thermal fluctuations. In supercooled states, $S(k, \Delta t)$ deviates from the true displacement correlation, showing the elastic-to-viscous crossover at a time scale of $\tau(k) = \eta(k)/G(k)$. On the other hand, for $\Delta t \lesssim \tau_\alpha$, $\hat{S}(k, \Delta t)$ can approximate the true displacement correlation, but can hardly capture the viscous dissipation. This discrepancy between $\hat{S}(k, \Delta t)$ and $S(k, \Delta t)$ represents a direction for constructing complete continuum mechanics.

Before closing, we present the following remarks. (i) In Fig. 5 in Appendix, we also show the longitudinal displacement correlation. For $\mathbf{u}_\mathbf{k}(\Delta t)$ [Eq. (2)], contrary to the transverse component, the elastic-to-viscous crossover does not occur at time scales of the shear-stress relaxation time. As schematically shown in Fig. 3, with regard to a hypothetical surface set in the system, ther-

mally vibrating particles crossing the surface do not have a perpendicular component of the net displacement between two crossing events. Therefore, a significant volumetric displacement is not caused for time scales smaller than τ_α , which is identified with the shear stress relaxation time in this study. In other words, the longitudinal displacement is only associated with material-mass flows [25, 29, 30]. Notably, the relaxation time of density fluctuations is systematically longer than the shear-stress relaxation time [29]. Please refer to Appendix for details. (ii) In other model glass formers (both strong and fragile), our preliminary simulations also show similar wavenumber dependence of the shear viscosity. For example, in silica (using the van Beest-Kramer-van Santen potential [31]), $\eta(k) \sim \eta$ for $k\xi_\eta \lesssim 1$, while $\eta(k) \sim k^{-3.3}$ for $k\xi_\eta \gtrsim 1$. However, in the Gaussian core model [32], $\eta(k)$ shows completely different behavior: for a wide temperature range, $\eta(k)$ approaches its macroscopic ($k = 0$) value already at the particle length scale and thus has a much steeper k -dependence, whose behavior is similar to that obtained from the calculation based on mode coupling theory (MCT) [9], which is consistent with the results of Ref. [33], where MCT qualitatively describes the dynamic properties of the Gaussian core model. (iii) How the present mechanism of viscous transport is related to the acoustic properties in supercooled liquids, glasses, and crystals may be interesting to study. For this purpose, the detailed physical properties of $\eta(k, \omega)$ or $\hat{\zeta}_\ell(\omega)$ should be revealed including rather high-frequency regimes. These issues will be addressed in future studies.

Acknowledgments

This work was supported by KAKENHI (Grants No. 26103507, 25000002, and 20508139), the JSPS Core-to-Core Program “International research network for non-equilibrium dynamics of soft matter”, and the special fund of Institute of Industrial Science, The University of Tokyo.

Appendix A: Simulation Models

In this study, we used the simple model of Ref. [10, 11]. The i -th and j -th particles interact via the following soft-core potentials

$$U(r_{ij}) = \epsilon \left(\frac{s_{ij}}{r_{ij}} \right)^{12}, \quad (\text{A1})$$

where $s_{ij} = (s_i + s_j)/2$, with s_i being the i -th particle’s size, and r_{ij} is the distance between the two particles. For supercooled liquids and glasses, we considered a three-dimensional binary mixture of large (A) and small (B) particles [10, 11]. The mass and size ratios are $m_B/m_A = 2$ and $s_B/s_A = 1.2$, respectively. The units for the length and time are s_A and $(m_A s_A^2/\epsilon)^{1/2}$, respectively. The total

number of particles was $N = N_A + N_B = 40000$, and $N_A/N_B = 1$. The temperature T was measured in units of ϵ/k_B . The fixed particle number density and the linear dimension of the system were $N/V = 0.8/s_A^3$ and $L = 36.84$, respectively.

On the other hand, for crystals, the following three dimensional monodisperse system was considered: the units for the length, time, and energy were also s_A , $(m_A s_A^2/\epsilon)^{1/2}$, and ϵ/k_B , respectively. The total number of particles was $N = 32000$. The number density and the linear dimension of the system were $N/V = 1.1/s_A^3$ and $L = 30.76$, respectively. With this setting, perfect face-centered cubic (FCC) crystal states were realized at $T = 0.08$ and 0.267 . All the simulations were performed using velocity Verlet algorithms in the NVE ensemble [12].

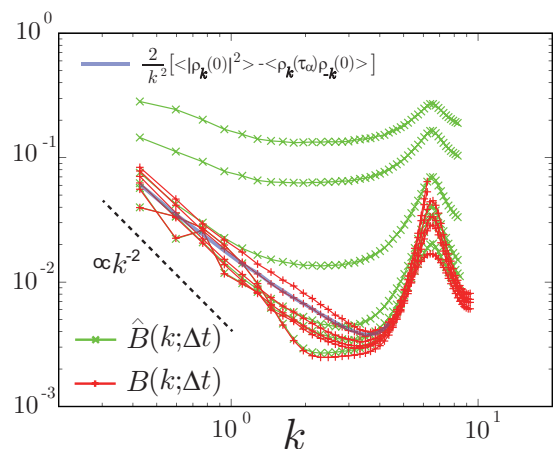


FIG. 5: (Color online) $\hat{B}(k; \Delta t)$ (green curve) and $B(k; \Delta t)$ (red curve) in a supercooled state ($T = 0.275$) at $\Delta t/\tau_\alpha = 5 \times 10^{-4}$, 2×10^{-3} , 2×10^{-2} , 2×10^{-1} , 1, and 2 (from bottom to top). Here, τ_α is defined as the macroscopic shear-stress relaxation time. The blue curve represents $(2/k^2)[\langle |\rho_{\mathbf{k}}(0)|^2 \rangle - \langle \rho_{\mathbf{k}}(\Delta t) \rho_{-\mathbf{k}}(0) \rangle]$ at $\Delta t = \tau_\alpha$. For $\Delta t \lesssim 0.1\tau_\alpha$, $\hat{B}(k; \Delta t)$ and $B(k; \Delta t)$ behave similarly. However, for larger Δt , the difference between $\hat{B}(k; \Delta t)$ and $B(k; \Delta t)$ becomes significant. The observed difference may be reduced by using the time-averaged or inherent-state positions instead of $\mathbf{r}_\lambda(0)$ in Eq. (1) in the main text.

Appendix B: The longitudinal displacement correlations

In Fig. 5, we show the longitudinal-displacement correlation: $\hat{B}(k; \Delta t) = \langle |\hat{\mathbf{u}}_{\mathbf{k}}^\parallel(\Delta t)|^2 \rangle$ and $B(k; \Delta t) = \langle |\mathbf{u}_{\mathbf{k}}^\parallel(\Delta t)|^2 \rangle$, where $\hat{\mathbf{u}}_{\mathbf{k}}^\parallel$ and $\mathbf{u}_{\mathbf{k}}^\parallel$ are the longitudinal components of $\hat{\mathbf{u}}_{\mathbf{k}}$ and $\mathbf{u}_{\mathbf{k}}$, respectively, at the same condition for that in Fig. 1 in the main text. We find differences between the longitudinal and transverse displacements, as well as different behaviors between $\hat{\mathbf{u}}_{\mathbf{k}}(\Delta t)$ and $\mathbf{u}_{\mathbf{k}}(\Delta t)$. Here, we would like to point out that $B(k; \Delta t)$

does not show the elastic-to-viscous crossover even at $\Delta t \sim \tau_\alpha$. As discussed in the main text, large changes in $B(k; \Delta t)$ are only associated with significant mass transfers or density exchanges. From the continuity equation, $B(k; \Delta t)$ is directly related to the density fluctuations as

$$B(k; \Delta t) = \frac{2}{k^2} [\langle |\rho_{\mathbf{k}}(0)|^2 \rangle - \langle \rho_{\mathbf{k}}(\Delta t) \rho_{-\mathbf{k}}(0) \rangle], \quad (\text{B1})$$

where $\rho_{\mathbf{k}}(t)$ is the density fluctuation at time t in Fourier space.

Appendix C: The k -dependent viscosity

Here, we describe the general formalism used to obtain $\eta(k)$. We start from the following generalized hydrodynamic equation [22, 23],

$$\frac{\partial}{\partial t} \mathbf{j}^\perp = (\nabla \cdot \overleftrightarrow{\boldsymbol{\sigma}}_{\text{vis}})^\perp + \boldsymbol{\theta}^\perp, \quad (\text{C1})$$

where $\mathbf{j}^\perp(\mathbf{r}, t)$ is the transverse momentum current, $\boldsymbol{\theta}^\perp(\mathbf{r}, t)$ is the transverse random force, and $\overleftrightarrow{\boldsymbol{\sigma}}_{\text{vis}}(\mathbf{r}, t)$ is the (transverse) viscous shear stress tensor that is given by $\overleftrightarrow{\boldsymbol{\sigma}}_{\text{vis}}(\mathbf{r}, t) = \int dt' \int d\mathbf{r}' \eta(|\mathbf{r} - \mathbf{r}'|, t - t') \overleftrightarrow{\boldsymbol{\kappa}}^\perp(\mathbf{r}', t')$ with a strain rate tensor of $\overleftrightarrow{\boldsymbol{\kappa}}^\perp(\mathbf{r}, t) = \nabla \mathbf{v}^\perp + (\nabla \mathbf{v}^\perp)^\dagger$. Here, $\mathbf{v}^\perp(\mathbf{r}, t)$ is the transverse velocity, and $\eta(|\mathbf{r} - \mathbf{r}'|, t - t')$ is a response function that represents the spatio-temporal nonlocal viscoelastic response. In k space, the above equation is expressed as

$$\frac{\partial}{\partial t} \mathbf{j}_{\mathbf{k}}^\perp(t) = -\frac{k^2}{\rho_m} \int dt' \eta(k, t - t') \mathbf{j}_{\mathbf{k}}^\perp(t') + \boldsymbol{\theta}_{\mathbf{k}}^\perp(t), \quad (\text{C2})$$

where ρ_m is the average mass density. Here, the Fourier transform of an arbitrary function, $f(\mathbf{r})$, is defined by $f_{\mathbf{k}} = \int d\mathbf{r} e^{-i\mathbf{k} \cdot \mathbf{r}} f(\mathbf{r})$. The microscopic expression of $\mathbf{j}_{\mathbf{k}}^\perp(t)$ is given by $\mathbf{j}_{\mathbf{k}}^\perp(t) = (1/\sqrt{N}) \sum_\lambda^N m_\lambda \mathbf{v}_\lambda^\perp(t) e^{i\mathbf{k} \cdot \mathbf{r}_\lambda(t)}$, where $\mathbf{v}_\lambda^\perp(t)$ is the transverse part of the velocity of particle i and thus satisfies $\mathbf{v}_\lambda^\perp(t) \cdot \mathbf{k} = 0$. Then, the autocorrelation function is defined as $C(k, t) = \langle \mathbf{j}_{\mathbf{k}}^\perp(t) \cdot \mathbf{j}_{-\mathbf{k}}^\perp(0) \rangle$,

whose time evolution is described by $(\partial/\partial t)C(k, t) = -(k^2/\rho_m) \int dt' \eta(k, t - t') C(k, t')$. Here, we make use of the relation $\langle \boldsymbol{\theta}_{\mathbf{k}}^\perp(t) \cdot \mathbf{j}_{-\mathbf{k}}^\perp(t') \rangle = 0$. The resulting (k, ω) dependence of the shear viscosity can be expressed as

$$\eta(k, \omega) = \frac{\rho_m}{k^2 \tilde{C}(k, \omega)} [-i\omega \tilde{C}(k, \omega) + C(k, 0)], \quad (\text{C3})$$

where $\tilde{C}(k, \omega) = \int_0^\infty dt e^{-i\omega t} C(k, t)$. The nonlocal viscoelasticity is characterized by the complex shear modulus, $G^*(k, \omega) = G'(k, \omega) + iG''(k, \omega) = i\omega \eta^*(k, \omega)$, where $G'(k, \omega)$ and $G''(k, \omega)$ are the so-called storage and loss moduli, respectively. The storage modulus represents the elastic response, whereas the loss modulus represents the dissipative viscous response. In the low-frequency limit ($\omega \rightarrow 0$), the k -dependent shear viscosity is obtained as

$$\eta(k) = \lim_{\omega \rightarrow 0} \frac{G''(k, \omega)}{\omega} = \frac{\rho_m}{k^2} \left[\int_0^\infty dt \frac{C(\mathbf{k}, t)}{C(\mathbf{k}, 0)} \right]^{-1}. \quad (\text{C4})$$

More specifically, $\eta(k) \cong G''(k, \omega)/\omega$ for $\omega\tau(k) \ll 1$ [9].

The transverse displacement correlation is given as,

$$\begin{aligned} S(k; \Delta t) &= \langle |\mathbf{u}_{\mathbf{k}}^\perp(\Delta t)|^2 \rangle \\ &= \int_0^{\Delta t} ds \int_0^{\Delta t} ds' \langle \mathbf{v}_{\mathbf{k}}^\perp(s) \cdot \mathbf{v}_{-\mathbf{k}}^\perp(s') \rangle \\ &\cong \frac{1}{\rho_m^2} \int_0^{\Delta t} ds \int_0^{\Delta t} ds' C(k, s - s'). \end{aligned} \quad (\text{C5})$$

With a wavenumber k and a sufficiently large $\Delta t (\gg \tau(k))$, we obtain Eq. (5) in the main text as

$$S(k; \Delta t) \cong \Delta t \frac{4T}{k^2 \eta(k)}. \quad (\text{C6})$$

Here, we make use of the equipartition law: $C(k, 0) = 2T\rho_m$.

-
- [1] L.D. Landau and E.M. Lifshitz, *Fluid Mechanics* (Pergamon Press, New York, 1959).
- [2] L.D. Landau and E.M. Lifshitz, *Theory of Elasticity* (Pergamon Press, New York, 1973).
- [3] K. Binder and W. Kob, *Glassy Materials and Disordered Solids* (World Scientific, Singapore, 2005).
- [4] J.C. Dyre, Rev. Mod. Phys. **78**, 953 (2006).
- [5] R. G. Larson, *The Structure and Rheology of Complex Fluids* (Oxford University Press, Oxford, 1999).
- [6] J. Kim and T. Keyes, J. Phys. Chem. B **109**, 21445 (2005).
- [7] A. Furukawa and H. Tanaka, Phys. Rev. Lett. **103**, 135703 (2009).
- [8] R. M. Puscasu, B. D. Todd, P. J. Daivis, and J. S. Hansen J. Chem. Phys. **133**, 144907 (2010).
- [9] A. Furukawa and H. Tanaka, Phys. Rev. E. **84**, 061503 (2011).
- [10] B. Bernu, Y. Hiwatari, and J.P. Hansen, Phys. C: Solid State Physics, **18**, L371-376 (1985).
- [11] B. Bernu, J.P. Hansen, Y. Hiwatari, and G. Pastore, Phys. Rev. A **36**, 4891 (1987).
- [12] D. C. Rapaport, *The Art of Molecular Dynamics Simulation* (Cambridge University Press, Cambridge, 2004).
- [13] E. Flenner and G. Szamel, Phys. Rev. Lett. **114**, 025501

- (2015).
- [14] C.L. Klix, F. Ebert, F. Weysser, M. Fuchs, G. Maret, and P. Keim, *Phys. Rev. Lett.* **109**, 178301 (2012).
- [15] Because the Eulerian velocity field $\mathbf{v}_{\mathbf{k}}$ is identified with the Lagrange derivative of the Eulerian displacement field, Eq. (2) does not describe the true displacement.
- [16] P. M. Chaikin and T. C. Lubensky, *Principles of Condensed Matter Physics*, (Cambridge Univ. Press, Cambridge, 1995).
- [17] Here, the elastic free energy and the shear stress tensor associated with the transverse displacement fluctuations are assumed to be given as $F_{\text{el}} = (1/2) \int_{\mathbf{k}} [G(k) |\mathbf{k} \hat{u}_{\mathbf{k}}^{\perp} + (\mathbf{k} \hat{u}_{\mathbf{k}}^{\perp})^{\dagger}|^2]$ and $G(k) [i\mathbf{k} \hat{u}_{\mathbf{k}}^{\perp} + (i\mathbf{k} \hat{u}_{\mathbf{k}}^{\perp})^{\dagger}]$, respectively.
- [18] B. Illing, S. Fritschi, D. Hajnal, C. Klix, P. Keim, and M. Fuchs *Phys. Rev. Lett.* **117**, 208002 (2016).
- [19] S. Fritschi and M. Fuchs, *J. phys., Condens. matter.* **30**, 024003 (2018).
- [20] M. Maier, A. Zippelius, and M. Fuchs, *J. Chem. Phys.* **149**, 084502 (2018).
- [21] L. Klochko, J. Baschnagel, J. P. Wittmer, and A. N. Semenov *Soft Matter* **33**, 6835 (2018).
- [22] J.P. Boon and S. Yip, *Molecular Hydrodynamics* (Dover, Newyork, 1991).
- [23] J.P. Hansen and I.R. McDonald, *Theory of Simple Liquids* (Academic Press, Oxford, 1986).
- [24] $\hat{S}(k; \Delta t) \sim k^{-2}$ indicates r^{-1} correlation in real space, leading to $\langle \hat{U}_{\ell}^2 \rangle \sim \ell^{-1}$. In Fig. 2, $|b|$ is slightly larger than 1 and shows a small dependence on Δt .
- [25] A. Furukawa, *J. Stat. Mech.* 084001 (2019).
- [26] A. Furukawa, *Phys. Rev. E* **87**, 062321 (2013).
- [27] Although in practice particles interact with each other, the estimation of D_{ℓ} does not depend on the interaction details; namely, the interaction effects are simply reflected in ω_0 and a .
- [28] The non-local elastic and hydrodynamic interactions are assumed to be renormalized in $\zeta_{\ell}(t)$
- [29] A. Furukawa and H. Tanaka, *Phys. Rev. E* **94**, 052607 (2016).
- [30] A. Furukawa, *Phys. Rev. E* **97**, 022615 (2018).
- [31] B.W.H. van Beest, G.J. Kramer, and R.A. van Santen, *Phys. Rev. Lett.* **64**, 1955 (1990).
- [32] F. H. Stillinger, *J. Chem. Phys.* **65**, 3968 (1976).
- [33] A. Ikeda and K. Miyazaki, *Phys. Rev. Lett.* **106**, 015701 (2011).